

Geothermal Exploration With Hyperspectral Data in the Carson Sink, Nevada

Chris Kratt, Wendy Calvin, Mark Coolbaugh
Great Basin Center for Geothermal Energy
University of Nevada, Reno
krattc@unr.nevada.edu

Abstract— Hyperspectral data was acquired over two geothermally active study areas in west-central Nevada. Carbonate and opaline sinter deposits associated with upwelling geothermal fluids were remotely mapped. Our results identified previously unmapped sinter outcrops and structurally controlled tufa, which both indicate fault traces acting as geothermal fluid pathways.

Keywords-component; hyperspectral, opal, sinter, geothermal, tufa, Nevada, VNIR/SWIR

I. INTRODUCTION

Geothermal energy production takes advantage of the earth as a natural heat source while emitting only about one-tenth of the greenhouse gasses emitted by gas or coal energy production [1]. Most geothermal systems occur along continental margins and regions of active tectonism. These regions also coincide with more densely distributed human populations, particularly in the developing world. In 1990 there were 5831 MegaWatts (MW) of geothermal power being generated at the global level and this number increased to 7974 MW by the year 2000 [2]. This increase in power production is in part a result of improved exploration techniques and production technology that takes advantage of lower temperature (<150° C) systems that were previously undeveloped.

All geothermal systems are the result of penetration of meteoric fluids into the crust, heating of those fluids, and consequent buoyant upflow of the fluids [3]. Many geothermal systems have active surface expressions such as fumaroles and hot springs. However, there are often unique mineralogic expressions associated with structurally controlled upwelling geothermal fluid where steaming ground or other obvious surface expressions are weaker.

Hyperspectral remote sensing data is a powerful exploration tool for the identification of discrete mineral endmember occurrences that can easily be missed by a field geologist and or undifferentiated by the human eye. It also allows for more rapid assessment of spatial phenomena that extend distances not easily traversed by foot. Not only does the presence of certain minerals potentially indicate a geothermal source but their spatial distribution is often a direct expression of subsurface controls [4]. Remote mapping results may then lead to more detailed exploration and

understanding of a geothermal source in addition to complementing any existing data. This paper discusses the application of hyperspectral data to geothermal exploration over two different sites in the Great Basin, Carson Sink, Nevada, USA.

II. GEOLOGIC BACKGROUND

We analyzed two separate study areas that each lie on the edges of the Carson Sink located about 50 km east of Reno in west-central Nevada. The Brady-Desert Peak geothermal field is located on Interstate 80 along the northwestern edge of the Carson Sink in the Hot Springs Mountains. The Salt Wells geothermal field is located off Highway 50 a few miles southeast of Fallon, Nevada on the southern edge of the Carson Sink against the Bunejug Mountains. Both study areas are in arid regions with consequently little vegetative cover, relief is less than 500 m.

Brady and Desert Peak geothermal systems each host a geothermal power plant operated by ORMAT Nevada Inc. and collectively produce 21 MW. Separated by about 5 km they are situated on the northeast-striking Brady and Rhyolite Ridge Faults, respectively. The primary lithologies in the Brady-Desert Peak area are diatomite, tufa, siltstone, limestone, shale and mafic to intermediate volcanics. The Bradys Fault is expressed by over 50 fumaroles in a sub-linear trend that extends for more than 2.3 km. In contrast, Desert Peak is considered a blind geothermal field due to weak surface manifestation [5].

With drilling at Salt Wells in the 1970s temperatures at depth around 124° C were encountered, however at that time these temperatures were not capable of power production. Energy initiatives and binary technology have more recently made Salt Wells the subject of renewed interest in geothermal development. Coolbaugh et al. (in press) have observed only a few small patches of warm ground as active signs of thermal activity. The lithologies in this area are limited to basalt, lacustrine and aeolian deposits. Morrison observed silicified sands but they were not mapped [6].

The ~13 million year old high shoreline of Pleistocene Lake Lahontan entirely submerged the Carson Sink before it evolved to its present status as a remnant basin [7]. The existence of Lake Lahontan promoted prolific precipitation of

the calcium carbonate deposit called tufa, which can form tall mounds (10+ meters) where cool sub-lacustrine spring waters mix with warmer lake water [8]. Fault controlled tufa deposition is observed as distinct linear mounds up to several meters high and wide along a number of Pleistocene and Holocene faults in the Lahontan Basin. Tufa deposition also commonly occurs as shoreline encrustations facilitated by microbial activity [9]. Lahontan paleo-shorelines are often easily mapped with spaceborne SWIR remote sensing data [10].

Rising silica-rich geothermal fluids gradually cool conductively and while still near boiling temperatures then become supersaturated where they encounter even cooler dilute lake water or the atmosphere [11]. Sinter is the rock formed by this epithermal precipitation and it is composed primarily of amorphous opal ($\text{SiO}_2 \cdot n\text{H}_2\text{O}$), which then diagenetically transforms chalcedony (fine-grained SiO_2). Opaline and chalcedonic sinters coincide with fault traces [12]. Brady-Desert Peak and Salt Wells both have outcrops of sinter, silcrete, silicified root casts and algal mats that were likely formed about 13 thousand years ago in shallow waters of Lake Lahontan along sub-lacustrine fault traces. Evidence for this type of depositional environment is supported by tufa overlying sinter and silcrete.

III. HYPERSPECTRAL INSTRUMENTS

On June 3, 2003 Hymap acquired 3m hyperspectral data over 130 km^2 centered on the Brady-Desert Peak area. Hymap is operated by the Hyvista Corporation and it acquires 126 channels of reflectance data from 0.4 to 2.5 μm . <http://www.hyvista.com>

Salt Wells hyperspectral data was acquired by the SpecTIR Corporation on June 11, 2004 and covers over 60 km^2 . The HyperSpecTIR (HST) instrument has 227 channels that acquire reflectance data from 0.45 to 2.45 μm and was also flown to achieve 3m spatial resolution. www.spectir.com/home.htm

Both of these instruments measure reflected light in the visible and shortwave infrared (VIS/SWIR) portions of the electromagnetic spectrum. It is also worth mentioning that their flight elevations of about 3000m above ground level can be adjusted to achieve spatial resolution better than 1m^2 .

IV. METHODOLOGY

Opal displays a broad spectral absorption feature centered on 2.25 μm (Fig. 1) due to the presence of water in the structure and Si-OH bonding [13]. We used this diagnostic absorption feature to remotely map surficially expressed silicified rocks associated with epithermal deposition. *A priori* field knowledge was used to select image spectra (Fig. 2) from sinter pixels that were then loaded into ENVI image

processing software Mixture Tuned Matched Filtering (MTMF) routine to produce a greyscale image in which the highest values were most closely matched to the input spectra [14].

We were also interested in structurally controlled tufa deposits. For this we employed an MTMF result with input carbonate image spectra. Alternatively a relative band depth (RBD) image was also generated by adding the channels that cover the shoulders of a strong 2.33 μm carbonate absorption feature and dividing them by the 2.33 μm channel itself.

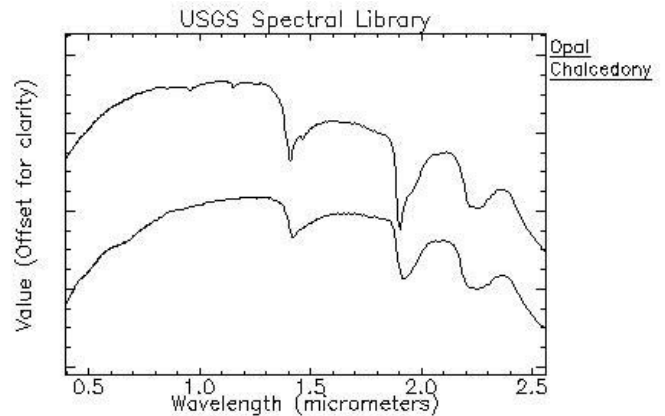


Figure 1

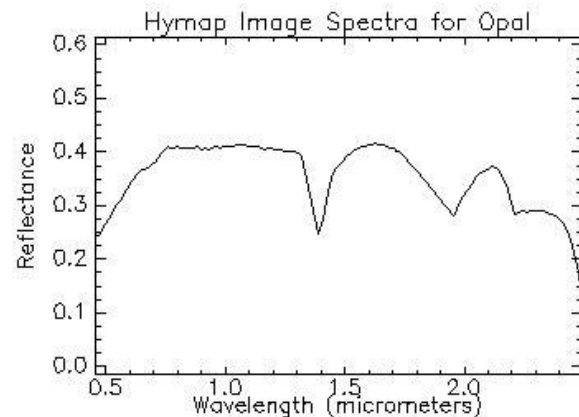


Figure 2

Higher values of the RBD image are associated with the most homogenous carbonate lithologies.

All mapping results were validated by rigorous ground-truthing with a field spectrometer and validation with the USGS spectral library [15]. Numerous X-ray diffraction analyses were also used for validation.

V. RESULTS

More liberal thresholds applied to the sinter MTMF result yielded a greater number of sinter false positives due to the presence of opal in other types of lithologies. Thick beds of lacustrine diatomite capped by a zone of silicified diatomite

were often mapped as sinter. This is explained by the fact that most diatoms commonly make their shells out of opaline silica [15]. The 2.25 μm opal absorption feature shifted to 2.20 μm with increasing presence of clay in the diatomite. One basalt outcrop near Desert Peak is particularly abundant in opal/chalcedonic inclusions and had several pixels that had very high values in the sinter MTMF result. Silicified sands display strong opal spectra when measured with the field spectrometer, however, they had more moderate MTMF values. In some cases it was necessary to use spatial subsets to map sinter that occurred primarily as float. Where the Bradys Fault loses its surface expression to the south there were false positives associated with hydrothermal alteration and silicification.

Although carbonate mapping with the MTMF result was very useful, qualitative analysis showed that the relative band depth image achieved a more robust result. Image spectra showed no distinction between Lahontan age tufa and 9 million year old limestone. However the deepest 2.33 μm carbonate absorption features were associated with limestone desert pavement. Sub-lacustrine tufa was not spectrally differentiable from other carbonates. Although, after all carbonates were mapped, characteristic linear and sharp crested morphology of structurally controlled sub-lacustrine tufa is more easily observed. This is in contrast to the more broadly and often topographically controlled distribution of other carbonates.

VI. CONCLUSIONS

Both instruments were capable of mapping sub-pixel occurrences of sinter and other types of silicification. Opal and chalcedony both have broad absorption features at 2.25 μm and have very similar spectral shapes throughout the rest of the wavelengths covered by these instruments. Because sinter is mapped primarily due to the presence of opal, other lithologies containing opal may be represented in an MTMF result as median values. Despite time spent field checking some false positives, previously unmapped sinter outcrops at both study areas were identified. At one location, a sinter outcrop covering over 60 m^2 straddled the road and appeared not much different from old beach sands, consequently going unmapped until recently recognized based on a match to sinter spectra.

Our sinter map of Brady-Desert Peak indicates a linear trend on-strike with, and extending from the southerly mapped limit of the Bradys Fault. This linear trend of sinter coincides with a structurally controlled tufa mound. The southerly end of the Bradys Fault has been thought to have continued southwestward over a broad saddle, new observations instead suggest a more westerly extension. Based in part on our remote and field mapping, new drilling and expansion of the Brady's geothermal field is currently underway. At Salt Wells our sinter map defines a broad northwest-trending zone extending over several kilometers. These observations at Salt

Wells will be important when combined with reconnaissance geologic mapping to be completed this summer.

ACKNOWLEDGMENTS

The authors gratefully acknowledge the support for this project from the U.S. Department of Energy, Assistant Secretary for Energy Efficiency and Renewable Energy, under DOE, DE-FG36-02ID14311.

REFERENCES

- [1] W. B. Goddard, and C. B. Goddard, Energy fuel sources and their contribution to recent global air pollution trends, *Geothermal Resources Council Transactions*, v. 14, pp. 643-649, 1990.
- [2] International Geothermal Association, <http://iga.igg.cnr.it/geoworld/geoworld.php?sub=elgen>
- [3] G. B. Arehart, M. F. Coolbaugh, and S. R. Poulsen, Geochemical characterization of geothermal systems in the Great Basin: Implications for exploration, exploitation, and environmental issues, *Proceedings, Annual Meeting, Reno, NV, Sept. 22-25, 2002*, *Geothermal Resources Council Transactions*, v. 26, p. 479-481.
- [4] B. A. Martini, Assessing hydrothermal system dynamics and character by coupling hyperspectral imaging with historical drilling data: Long Valley Caldera, CA, USA, *Proceedings 25th NZ Geothermal Workshop*, 2003.
- [5] W. R. Benoit, J. E. Hiner, and R. T. Forest, Discovery and geology of the Desert Peak Geothermal Field: a case history, *Nevada Bureau of Mines and Geology Bulletin* 97, p. 82, 1982.
- [6] R. B. Morrison, Lake Lahontan: geology of southern Carson Desert, Nevada: U. S. Geological Survey Professional Paper 401, p. 156, 1964.
- [7] K. Cupp, and K. D. Adams, Quaternary history, isostatic rebound and active faulting in the Lake Lahontan Basin, Nevada and California, *Friends of the Pleistocene Pacific Cell*.
- [8] T. C. Council, and P. C. Bennett, Geochemistry of ikaite formation at Mono Lake, California: implications for the origin of tufa mounds, *Geology*, v. 21, p. 971-974, 1993.
- [9] T. D. Ford, and H. M. Pedley, A review of tufa and travertine deposits of the world, *Earth-Science Reviews*, v. 41, no. 3-4, pp. 117-175, 1996.
- [10] C. B. Kratt, W. M. Calvin, and M. F. Coolbaugh, Possible extension of Brady's Fault identified using remote mapping techniques, *Geothermal Resources Council Transactions*, v. 27, pp. 653-656, 2003.
- [11] R. W. Renaut, W. B. Jones, J. J. Tiercelin, and C. Tartis, Sublacustrine precipitation of hydrothermal silica in rift lakes: evidence from Lake Baringo, central Kenya Rift Valley, *Sedimentary Geology*, v. 148, pp. 235-257, 2002.
- [12] D. G. White and T. C. Sandberg, Rocks, structure, and geologic history of Steamboat Springs thermal area, Washoe County, Nevada, *USGS Professional Paper* 458-B pp. 63, 1964.
- [13] G. A. Swayze and R. F. Kokalay, Spectral detection of a 2.25-micron absorption band in impactites formed from silicious sediments; a new way to locate shocked materials, *Abstract with Programs, Geological Society America*, v. 31, no. 7, p. 122, 1999.
- [14] J. W. Boardman and F. A. Kruse, Automated spectral analysis: a geologic example using AVIRIS data, north Grapvine Mountains, Nevada, *Proceedings, Tenth Thematic Conference on Geologic Remote Sensing*, Environmental Research, Institute of Michigan, Ann Arbor, MI, pp. 1-407 - 1418, 1994.
- [15] R. N. Clark, G. A. Swayze, A. J. Gallaher, T. V. V. King, and W. M. Calvin, The U. S. G. S. Geological Survey, Digital Spectral Library: version 1: 0.2-3.0 microns, U. S. Geological Survey Open File Report 93-592, 1993.
- [16] E. R. Segnit and J. B. Jones, The nature of opal: nomenclature and constituent phases, *Journal of the Geological Society of Australia*, v. 18 no. 1, pp. 57-67, 1971.